Effects of stimulated emission on transport in terahertz quantum cascade lasers based on diagonal designs

I. Bhattacharya,[1] C. W. I. Chan,[2,a)] and Q. Hu[2]
[1]*Department of Electrical Engineering, Indian Institute of Technology Bombay, Mumbai, Maharashtra, India*
[2]*Department of Electrical Engineering and Computer Science and Research Laboratory of Electronics, Massachusetts Institute of Technology, Cambridge, MA 02139, USA*

(Received 18 November 2011; accepted 13 December 2011; published online 6 January 2012)

A hybrid Monte Carlo-density matrix transport simulator is used to analyze the transport properties of resonant-phonon type terahertz quantum cascade lasers. By comparing calculated and experimental results, the importance of stimulated emission to the interpretation of experimental data is highlighted, particularly for devices based on diagonal radiative transitions. Finally, we discuss the absence of mode competition effects on transport. © *2012 American Institute of Physics*. [doi:10.1063/1.3675452]

Quantum cascade lasers (QCLs) are promising sources of coherent terahertz radiation,[1] but unfortunately they require cryogenic operation. To address this issue, recent research has focused on designs employing diagonal radiative transitions to increase the upper-laser level lifetime, whose rapid decrease versus temperature is believed to be a major obstacle to improving maximum lasing temperatures. Indeed, the present temperature record of 186 K is achieved from a resonant-phonon type THz QCL employing a diagonal radiative transition.[2] Inspired by this result, we have attempted to improve temperature performance through designing QCLs with even more diagonal radiative transitions.[3] In this letter, we show experimentally that such highly diagonal devices exhibit unique transport properties not seen in traditional designs employing vertical radiative transitions. Furthermore, we show in our simulations that stimulated emission is essential to explain these peculiar transport properties. We compare theoretical transport calculations with experimental data obtained from devices reported in Refs. 2–4.

Given the importance of coherence in QCL tranport,[5,6] we employ a hybrid Monte-Carlo/Density matrix method (MCDM).[7] In this approach, electrons evolve coherently between QCL periods through a quantum Liouville operator calculated in a basis of tight-binding subband states localized within a QCL period. Scattering between the tight-binding states within each period is handled using an ensemble Monte Carlo method (EMC), with scattering rates determined by Fermi's golden rule.

The electron-photon interaction can in principle be included through the evolution of the density matrix. Such a treatment enables modeling of important effects such as nonlinear gain and gain splitting.[6,8,9] However, for the subject of interest in this paper (DC transport), we treat the electron-photon interaction through the simpler rate-equation approach of Ref. 10, where each optical mode is tracked by its frequency and classical intensity, and the overall optical field is treated as an EMC scattering mechanism. Rather than calculating level broadening, we simply assume a 1 THz Lorentzian FWHM for all optical transitions. Interactions between the optical field and the density matrix coherences are ignored.

Figure 1 compares calculated and experimental current-voltage (*I-V*s) characteristics for a diagonal device (OWI222G from Ref. 2) and a vertical device (FL183R from Ref. 4). For the vertical device, reasonable agreement with experimental data occurs both with and without inclusion of lasing in the MCDM calculation. But for the diagonal device, inclusion of lasing is essential for a good agreement. These results indicate that lasing can be important for current conduction, in addition to causing a discontinuous jump in dI/dV.[11] This is supported by other recent experimental results,[12] as well as studies of midinfrared QCLs.[13]

In particular, lasing strongly affects the appearance of negative differential resistance (NDR). Typical THz QCLs based on the resonant-phonon design normally exhibit a pronounced NDR close to design bias. This is usually attributed to the cessation of resonant tunneling caused by misalignment of the injector and upper-laser levels. However, the non-lasing OWI222G device in Fig. 1(a) barely shows any NDR. This is consistently observed in diagonal designs,[3] and in extreme cases NDR can be wholly absent without lasing (e.g., incidental resonant-tunneling type lasing observed in device in Ref. 15).

This may be explained by the diagonality of the lasing transition. Transport through the injector barrier is qualitatively described by the Kazarinov-Suris expression for current tunneling,

$$J = \frac{eN}{2\tau}\frac{4\Omega^2\tau\tau_{||}}{4\Omega^2\tau\tau_{||} + \omega_{21}^2\tau_{||}^2 + 1}, \tag{1}$$

where Ω is the coupling between the subbands across the barrier, τ is the upper-level lifetime, $\tau_{||}$ is the decoherence time between the injector and upper-level, and ω_{21} is the energy misalignment between the two.[16] Equation (1) describes a Lorentzian centered at $\omega_{21} = 0$, with width proportional to $\sqrt{4\Omega^2\tau\tau_{||} + 1}$. Therefore, the prominence of NDR is determined by whether the upper-level lifetime or

a)Electronic mail: icwchan@mit.edu.

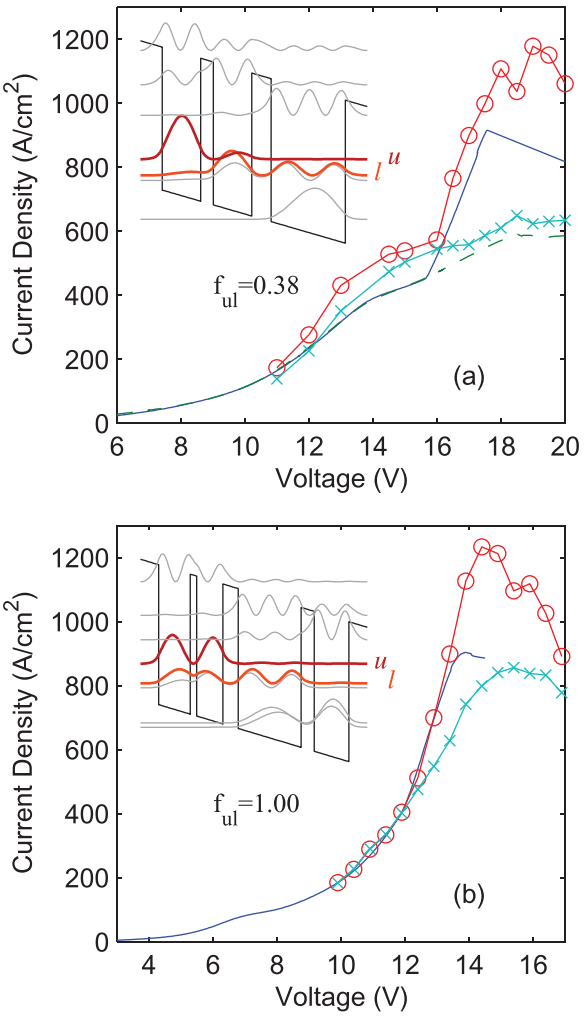

FIG. 1. (Color online) Calculated and experimental *I-V* data for designs of (a) Ref. 2, (b) Ref. 4, assuming 20 cm^{-1} cavity loss[14] and a 10 K lattice temperature. (o), MCDM with lasing; (x), MCDM without lasing; solid lines, measured from a lasing device; dashed lines, measured from a non-lasing device (not available for (b)). MCDM data is fitted to experimental data with constant voltage offsets to account for voltage drops at the contacts (+7 V in (a), +3.9 V in (b)). Upper (u) and lower (l) subbands in band diagrams are highlighted. Lasing was suppressed in the non-lasing device of (a) by covering the device in Stycast 2850 glue to increase optical losses.

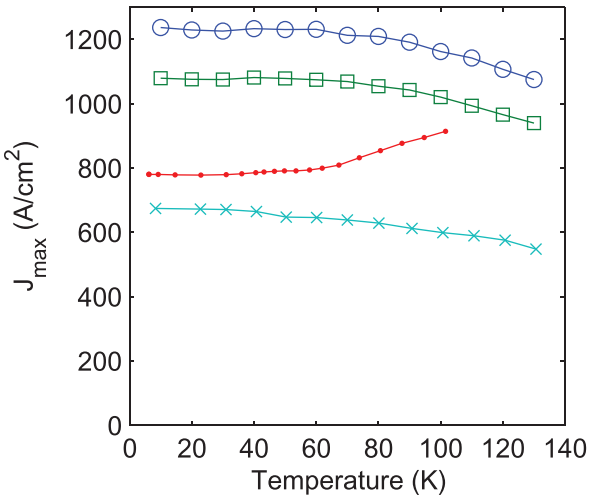

FIG. 2. (Color online) J_{max} as a function of temperature for (o), vertical design, Ref. 4, MCDM; (•), vertical design, experimental data; (□), diagonal design (OWI222G-M1 in Ref. 3), MCDM; (x), diagonal design, experimental data. Experimentally, a clear drop in J_{max} is seen in the diagonal design but not in the vertical design.

resonant tunneling is the bottleneck to transport. Resonant tunneling limited transport corresponds to $\tau \ll 1/\Omega^2\tau_{||}$ (sharp resonance, sharp NDR), whereas lifetime-limited transport corresponds to the case $\tau \gg 1/\Omega^2\tau_{||}$ (broad resonance, mild NDR). In the latter regime—to which diagonal designs belong—lasing can dramatically alter transport through reduction of the upper-level lifetime, effectively switching from the $\tau \gg 1/\Omega^2\tau_{||}$ regime to the $\tau \ll 1/\Omega^2\tau_{||}$ regime.

A peculiar consequence is that if transport is strongly limited by the upper-level lifetime, the maximum current density prior to the onset of NDR, J_{max}, will *decrease* with temperature. This reflects the reduction of dynamic range as temperature rises and subsequent decrease in stimulated emission (a similar drop is predicted due to an increasing waveguide loss[6]). Figure 2 compares experimental and calculated J_{max} versus temperature for FL183R (oscillator strength ~1) and OWI222G-M1 (a version of OWI222G modified to have an oscillator strength of 0.25).[3] Although the current density is over-predicted (perhaps due to insufficient treatment of dephasing or slight errors in MBE growth), the simulated J_{max} including the effect of stimulated emission shows a clear decrease with increasing operating temperature. This trend agrees well with experimental results from the diagonal design. For the vertical design, in which J_{max} is not limited by the upper-level lifetime, the experimental J_{max} is flat at low temperature and increases at higher temperatures (Fig. 2). The lack of decrease of J_{max} with temperature may be due to leakage channels (e.g., to continuum) that are absent in our modeling. Compared to the vertical design, the upper-level wavefunctions of the diagonal designs are more localized near the injection barrier, reducing such leakages; this could explain why our model agrees better with experiment for the diagonal design of OWI222G-M1. In any case, the anomalous decrease of J_{max} with temperature is explicable only by including the stimulated emission in calculations.

Finally, we note that although we are principally interested in the MCDM steady state, relevant physical information exists in the initial simulation transients. This is because EMC simulations converge through the actual physics of scattering. In particular, we examine mode competition during initial transients. Figure 3(a) shows the evolution of mode intensities in a multimode simulation. These converge much slower than the subband populations shown in Fig. 3(b), which reach steady-state in ~20 ps. The slow convergence of modal dynamics is observed in experimental studies of mid-infrared external cavity QCLs (Ref. 17) and is consistent with similar computational findings in Ref. 10.

This is intuitive, as a spectrally dense, multi-mode structure results in neighboring optical modes seeing approximately the same gain as the dominant lasing mode. The discrepancy in convergence time between photon and electron dynamics is resolved by observing in Fig. 3(a) that the *total* intensity converges much more rapidly than the intensity of any one mode. More rigorously, the *sum* of electron-

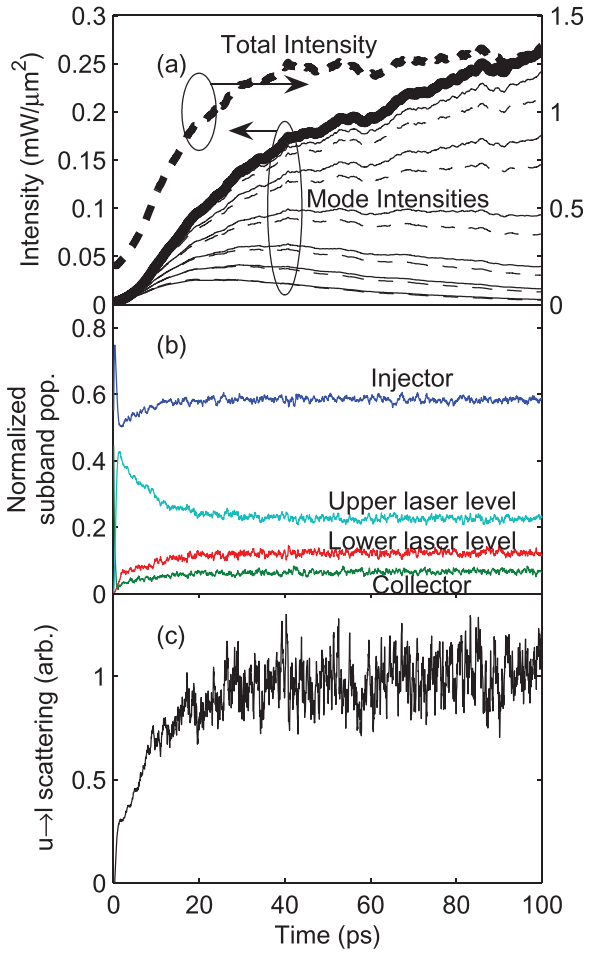

FIG. 3. (Color online) (a) Temporal evolution of optical modes for the design of Ref. 2. Solid bold line is the intensity of the dominant mode ω_0; modes at frequencies $\omega_m < \omega_0$ are solid, modes at frequencies $\omega_m > \omega_0$ are dashed. Modes are spaced by 40 GHz between 2 THz and 5 THz (for clarity, not all modes are plotted). Total intensity is the bold dashed line, plotted on an expanded scale. (b) Corresponding subband populations. (c) Upper- to lower-laser level optical scattering rate. The populations, total intensity, and total scattering rate converge within ~20 ps, but the mode intensities take much longer.

photon scattering rates across all optical modes converges much faster than that due to any individual mode. The rate of optical transitions between the upper- and lower-laser levels (ignoring state blocking for the moment) is given by

$$W_{ul} = V \sum_m \frac{I_m}{\hbar\omega_m} g_{ul}(\omega_m) \approx V \sum_m \frac{I_m}{\hbar\omega_m} g(\omega_m), \qquad (2)$$

where V is the active region volume, I_m and ω_m and the modal intensities and frequencies, and g is the gain, which is assumed to be dominated by the lasing transition. In contrast to the individual mode intensities, this rate converges rapidly (Fig. 3(c)). A practical consequence is that optical convergence of each individual mode is not necessary for accurate simulation of transport; transport can be efficiently simulated using a single lasing mode placed at peak gain.

In conclusion, we have used MCDM simulations combined with a semiclassical rate equations approach for electron-photon interactions to simulate transport including the effect of stimulated emission in THz QCLs. We demonstrate that lasing is crucial for explaining QCL transport, in particular for diagonal laser designs. We also demonstrate theoretically that photon dynamics due to mode competition takes significantly longer to converge than the electron dynamics of transport.

We gratefully acknowledge funding from NASA and NSF. C. W. I. Chan would further like to thank NSERC for his first year scholarship during which part of this research was conducted.

[1]B. S. Williams, Nat. Photonics **1**, 517 (2007).
[2]S. Kumar, Q. Hu, and J. L. Reno, Appl. Phys. Lett. **94**, 131105 (2009).
[3]C. W. I. Chan, M.S. thesis, Department of Electrical Engineering and Computer Science, Massachusetts Institute of Technology, 2010 (unpublished).
[4]B. Williams, S. Kumar, Q. Hu, and J. Reno, Electron. Lett. **42**, 89 (2006).
[5]C. Weber, A. Wacker, and A. Knorr, Phys. Rev. B **79**, 165322 (2009).
[6]S. Kumar and Q. Hu, Phys. Rev. B **80**, 245316 (2009).
[7]H. Callebaut and Q. Hu, J. Appl. Phys. **98**, 104505 (2005).
[8]J. B. Khurgin, Y. Dikmelik, P. Q. Liu, A. J. Hoffman, M. D. Escarra, K. J. Franz, and C. F. Gmachl, Appl. Phys. Lett. **94**, 091101 (2009).
[9]E. Dupont, S. Fathololoumi, and H. C. Liu, Phys. Rev. B **81**, 205311 (2010).
[10]C. Jirauschek, Appl. Phys. Lett. **96**, 011103 (2010).
[11]C. Sirtori, F. Capasso, J. Faist, A. Hutchinson, D. Sivco, and A. Cho, IEEE J. Quantum Electron. **34**, 1722 (1998).
[12]R. Sharma, L. Schrottke, M. Wienold, K. Biermann, R. Hey, and H. T. Grahn, Appl. Phys. Lett. **99**, 151116 (2011).
[13]A. Mtys, P. Lugli, and C. Jirauschek, J. Appl. Phys. **110**, 013108 (2011).
[14]D. Burghoff, T.-Y. Kao, D. Ban, A. W. M. Lee, Q. Hu, and J. Reno, Appl. Phys. Lett. **98**, 061112 (2011).
[15]S. Kumar, C. W. I. Chan, Q. Hu, and J. L. Reno, Nat. Phys. **7**, 166 (2011).
[16]R. F. Kazarinov and R. A. Suris, Sov. Phys. Semicond. **5**, 707 (1971).
[17]B. Hinkov, Q. Yang, F. Fuchs, W. Bronner, K. Khler, and J. Wagner, Appl. Phys. Lett. **94**, 221105 (2009).